TITLE: Detection of early osteogenic commitment in primary cells using Raman spectroscopy

AUTHORS: Stephanie J. Smith, Roger Emery, Andrew Pitsillides, Claire E. Clarkin and Sumeet Mahajan

JOURNAL TITLE: Analyst

PUBLICATION DATE: May 2017

PUBLISHER: Royal Society of Chemistry

DOI: 10.1039/C6AN02469F

Royal
Veterinary
College
University of London

Detection of early osteogenic commitment in primary cells using Raman spectroscopy

Stephanie J. Smith[1], Roger Emery[2], Andrew Pitsillides[3], Claire E. Clarkin[1†*], Sumeet Mahajan[4†*].

[1]Department of Biological Sciences, University of Southampton, SO17 1BJ, U.K.
[2]Division of Surgery, Reproductive Biology and Anaesthetics, Imperial College London, U.K
[3]Department of Veterinary Basic Science, Royal Veterinary College, London, NW1 0TU, U.K.
[4]Department of Chemistry and the Institute for Life Sciences, University of Southampton SO17 1BJ, U.K.

*Correspondence to: s.mahajan@soton.ac.uk, c.e.clarkin@soton.ac.uk
† Authors contributed equally to this study

Abstract

Major challenges in the development of novel implant surfaces for artificial joints include osteoblast heterogeneity and the lack of a simple and sensitive *in vitro* assay to measure early osteogenic responses. Raman spectroscopy is a label-free, non-invasive and non-destructive vibrational fingerprinting optical technique that is increasingly being applied to detect biochemical changes in cells. In this study Raman spectroscopy has been used to obtain bone cell-specific spectral signatures and to identify any changes therein during osteoblast commitment and differentiation of primary cells in culture. Murine calvarial osteoblasts (COBs) were extracted and cultured and studied by Raman spectroscopy over a 14 day culture period. Distinct osteogenic Raman spectra were identified after 3 days of culture with strong bands detected for mineral: phosphate v_3 (1030 cm^{-1}) and B-type carbonate (1072 cm^{-1}), DNA (782 cm^{-1}) and collagen matrix (CH$_2$ deformation at 1450 cm^{-1}) and weaker phosphate bands (948 and 970 cm^{-1}). Early changes were detected by Raman spectroscopy compared to a standard enzymatic alkaline phosphatase (ALP) assay and gene expression analyses over this period. Proliferation of COBs was confirmed by fluorescence intensity measurements using the Picogreen dsDNA reagent. Changes in ALP levels were evident only after 14 days of culture and mRNA expression levels for ALP, Col1a1 and Sclerostin remained constant during the culture period. Sirius red staining for collagen deposition also revealed little change until day 14. In contrast Raman spectroscopy revealed the presence of amorphous calcium phosphate (945-952 cm^{-1}) and carbonated apatite (957-962 cm^{-1}) after only 3 days in culture and octacalcium phosphate (970 cm^{-1}) considered a transient mineral phase, was detected after 5 days of COBs culture. PCA analysis confirmed clear separation between time-points. This study highlights the potential of Raman spectroscopy to be utilised for the early and specific detection of proliferation and differentiation changes in primary cultures of bone cells.

1

1. Introduction

Studies of bone forming osteoblast cells have significant medical impact with stimulation of osteoblast formation and activation continuing to have wide clinical demand. Although bone exhibits some highly conserved factors in its development, remodelling and repair, it is also apparent that the response to many *in vivo* challenges is not always consistent in different regions of bone [1-3]. These observations suggest that osteoblast populations are inherently heterogeneous and support a current hypothesis that their identity is specific to their local environment [4]. In recent attempts to clinically improve the success of joint replacement much focus has been on the study of the bone cell-implant interface with the long term success of joint replacement relying on sufficient osteoblast adherence, proliferation and differentiation in promoting osseointegration in specific regions. [5-7]. Historically, successful osseointegration has been assessed post implantation radiographically. However the study of osteoblast activity *in vitro* on implant surfaces could improve the development of implant coatings and allow for more accurate predictions of posteoperative osseointegration success. While in this paper we study osteoblast activity on quartz cover slips it is relevant and will provide insight for implant surfaces, subsequent studies and their modelling.

Osteoblast cells derive from mesenchymal progenitors and transition to pre-osteoblasts before finally becoming bone forming osteoblasts [8]. The differentiation process of osteoblasts is often defined by the presence of these three different-stage cell types but their identities are not yet clearly defined. Early transgenic studies describe the genes required for osteoblast differentiation [9, 10]. It is now generally accepted that transcription factors Runx2, osterix and β-catenin are involved in the regulation of osteoblast differentiation [11]. Currently, identifying mesenchymal progenitor commitment to the osteoblast lineage is in the expression of Runx2 and osterix, at which point they are considered pre-osteoblasts [12, 13]. Mature osteoblasts are characterised by their ability to secrete large amounts of extracellular proteins including osteocalcin alkaline phosphatase (ALP) and type I collagen, the main constituents of osteoid matrix which forms prior to osteoblast commitment and

2

83 mineralisation [8, 14]. The final stage of bone formation is mineralisation which

84 is thought to initiate with the formation of hydroxyapatite (HA) crystals inside

85 matrix vesicles (MVs) which are 50-200 nm in diameter and bud from the

86 surface membrane of hypertrophic chondrocytes and osteoblasts [15-18].

87 Inorganic calcium (Ca^{2+}) and phosphate (Pi) ions accumulate inside MVs

88 instigating the breakdown of the MV membrane, releasing HA crystals into the

89 extracellular fluid where they propagate on the collagenous extracellular matrix

90 [16, 19-21]. Inorganic phosphate ions also play a key role in regulating

91 mineralisation.

92

93 During *in vitro* bone formation, expression of mature osteoblast specific genes

94 and subsequent mineralisation typically takes place between 14 to 28 days [22,

95 23]. An ability to detect and quantify osteoblast differentiation early during the

96 culture process is attractive in the comparative study of distinct osteoblast

97 populations and also clinically for evaluating growth on implant surfaces.

98 Raman spectroscopy, an optical vibrational finger-printing technique, is label-

99 free, non-invasive and non-destructive and can be a more sensitive means

100 compared to conventional biochemical methods to detect osteogenesis.

101

102 Raman spectroscopy has gained a lot of interest in recent years as a potential

103 diagnostic tool for detecting such early biochemical changes in cells [24].

104 Raman spectroscopy has also indeed been widely applied to characterise bone

105 and its constituents [25-27]. Its capability to detect bone nodule formation in *in*

106 *vitro* secondary cell cultures has also been demonstrated although under high

107 mineralisation conditions [28, 29]. Recently the application of Raman

108 spectroscopy to grade live osteosarcoma cells was also investigated by Chiang

109 *et al*, who measured levels of hydroxyapatite produced by osteosarcoma cell

110 lines, a possible measure of malignancy [30]. By characterising the Raman

111 signatures of different cell types, researchers have been able to apply this

112 technique to monitor the differentiation of stem cells with Raman effectively

113 monitoring the osteogenic differentiation of human mesenchymal stem cells

114 (hMSCS) from 7 days of *in vitro* culture [31]. Hung *et al* also used hMSCs to

115 investigate matrix formation as a measure of maturation of live hMSCs [32].

116 Although this paper has demonstrated the feasibility of using Raman

3

spectroscopy to quantitatively analyse hMSC maturity, here we perform a thorough investigation on primary osteoblast cells isolated directly from murine neonatal bone tissue, and have been able to detect and characterise spectral changes over 14 days of culture due to proliferation, differentiation and deposition of matrix in osteoblasts. Whilst Hung *et al* were unable to detect early amorphous forms of calcium phosphate, we were able to not only detect different transient mineral species, but also quantify changes over time. Moreover, we study osteoblast cultures in natural growth (physiological) rather than over-mineralising conditions most often used by Raman researchers studying similar bone cells or osteogenesis [29]. Furthermore, we show that these changes are observed by Raman spectroscopy earlier than typical enzymatic and gene expression assays. Our study therefore establishes Raman spectroscopy as a simple, label-free, non-invasive and non-destructive alternative tool for assessing primary bone cultures and early changes therein with many applications in the field of skeletal regeneration.

2. Materials and Methods

2.1 Reagents

All tissue culture reagents, including α Minimum essential medium (αMEM) (no. 22571) and fetal calf serum (FCS) (no. 102701) were purchased from Invitrogen Life Technologies (Paisley, UK). All other reagents were purchased from Sigma unless otherwise stated.

2.2 Isolation and culture of calvarial osteoblasts.

Primary mouse calvarial osteoblasts (COBs) were obtained by sequential enzyme digestion of excised calvarial bone from 4-day-old neonatal mice (c57/bl6) using a 4-step process (CCEC; [50]). The first digest (1 mg/ml collagenase type Ⅱ in HBSS for 10 min) was discarded. The following 3 digests (fraction 1, 1 mg/ml collagenase type Ⅱ in HBSS for 30 min; fraction 2, 4 mM EDTA in PBS for 10 min; fraction 3, 1 mg/ml collagenase type Ⅱ in HBSS for

4

30 min) were retained. During the final digestion, the cells obtained from fractions 1 and 2 were resuspended in αMEM supplemented with 10% heat-inactivated FCS (HI FCS), 5% gentamicin, 100 U/ml penicillin, 100 µg/ml streptomycin. The cells from fraction 3 were then combined with fractions 1 and 2 for expansion. The cells were cultured in 75 cm^2 flasks (6 calvaria/ flask) for 7 days in a humidified atmosphere of 5% CO_2-95% air at 37˚C until confluent.

Upon confluence COBs were either plated into 12 well tissue culture plates or quartz coverslips (UQG optics CFQ-1017 #No1.5, thickness: 0.17 mm, Ø 10) at density of 7900 cells/cm^2. Cells were cultured for 3, 5, 7 and 14 days in αMEM supplemented with osteogenic media containing 50µg/ml ascorbic acid (AA) and 2.5 mM β- Glycerophosphate (BGP). For Raman spectroscopy COBs were fixed with 4% w/v paraformaldehyde and stored in PBS prior to imaging.

2.3 Alkaline Phosphatase activity elution assay and staining

COBs for elution assay were grown in 12 well plates as described above, washed twice with PBS before treating with 100% ethanol for 1 minute. Fixative was removed and cells were washed twice in distilled water. P-nitrophenol substrate (1mg/ml) was then added to a working solution of 70% dH20, 20% 0.1M NaHCO3 and 10% 30mM $MgCl_2$, pH was adjusted to 9.5. 500 µl of working solution was added to each well and incubated for 30 minutes at 37°C. 2x200 µl of eluted solution was removed and pipetted into a 96 well plate. Absorbance was measured after 1 minute at 405 nm. Concentration of nmols/ml/minute was calculated using a standard curve of known concentrations of p-nitrophenol solution (0.05, 0.1, 0.15, 0.2, 0.25mM).

ALP activity was also visualised by histochemical staining at day 3, and 14. After fixation with methanol: acetone cells were rinsed then treated with naphthol AS-MX as a substrate and Fast blue to produce a coloured precipitate.

2.4 Sirius Red collagen staining

5

To visualise collagen deposition over time, Sirius red staining was performed at days 3, 5, 7 and 14. COBs were grown in 12 well plates at a density of 5 x 10^4 cells/well, with and without BGP and AA. After the desired culture period, cells were washed twice with PBS before fixing with 70% ethanol for 1 hour. After fixation, cells were dried at 37°C and stained with Sircol Dye Reagent (Biocolor, County Antrim, UK) for 1 hour. After staining, cells were washed with dH_2O and allowed to air dry.

2.5 RNA Extraction and cDNA synthesis

After removal of culture media and washing with PBS, COBs were disrupted with lysis buffer. Lysates were stored at -80°C before RNA extraction. Total RNA was isolated using Qiagen RNeasy Mini Kit according to the manufacturer's instructions. The RNA for each sample was determined using a Nanodrop UV-vis spectrophotometer. cDNA was synthesised using the RT2 First Strand Kit (Qiagen catalogue #330401). Osteogenesis array carried out using PAMM-026ZA-6 - RT² Profiler™ Mouse Osteogenesis PCR Array (Qiagen catalogue #33023). Used Bio-Rad/MJ Research Chromo4 thermal cycler. Thermal cycling conditions included a 10 minute HotStart DNA Taq activation step at 95°C, followed by 40 cycles of 95°C for 15 seconds and 55°C for 30 seconds. A melting curve was included with temperature increase from 65°C to 95°C with 0.2°C increments for 1 second.

2.6 Genomic DNA isolation and Picogreen assay

COBs for genomic DNA extraction were cultured in 6 well plates as described above. After desired culture period, medium was removed and cells were washed with PBS, before the addition of 250 µl Trypsin/EDTA. An equal volume of α- MEM medium was added to the cells after dissociation to neutralise the trypsin. COBs were transferred to an Eppendorf and centrifuged at 10,000 RPM for 5 minutes. Pelleted cells were resuspended in 200 µl PBS and PureLink™Genomic DNA MiniKit was used to isolate genomic DNA according to manufacturer's instructions.

Once genomic DNA was obtained, the Quant-iT™PicoGreen®dsDNA reagent, a fluoresecent nucleic acid stain was used to quantitate double stranded DNA

6

217 present in the genomic DNA isolated from COBs. The fluorescence assay was
218 measured with a Hitachi F2500 fluorescence spectrophotometer. Samples
219 were excited at 480 nm and fluorescence intensity was measured at 520 nm.
220 DNA concentration was determined from a previously generated standard
221 curve of known DNA concentrations (1 µg/ml, 100 ng/ml, 10 ng/ml, 1 ng/ml and
222 a blank of TE buffer only).

223

224 2. 7 Raman Spectroscopy

225

226 For Raman spectroscopy calvarial osteoblasts (COBs) were cultured for 3, 5, 7
227 and 14 days in osteogenic media (as previously described) on sterilised quartz
228 coverslips. Cells were washed with Dulbecco's phosphate buffered saline (PBS)
229 before fixing with 4% paraformaldehyde for 5 minutes at room temperature.
230 After fixation COBs were washed in PBS. Raman spectra were obtained using
231 a Renishaw® inVia Raman microscope with a 532 nm laser and a Leica 63x
232 (NA: 1:2) water immersion objective in combination with WIRE 3.4 software.
233 The diffraction limited spot size is ~300 nm. However, we note that the spectral
234 collection was not confocal. Therefore the signal was collected from a focal
235 volume defined by the spot size. For consistency Raman spectra were always
236 collected from single cells over the nucleus. The nucleus was selected as a
237 marker area as it was the most distinctly visible feature of cell in the brightfield
238 image. Spectra were acquired from 20 cells and for each spectrum 2
239 accumulations of 30 s exposure were collected.
240 Cosmic ray artefacts were removed using WiRE 3.4. Before plotting the spectra
241 they were processed using IRootLab, a MATLAB based toolbox for vibrational
242 spectroscopy. Prior to general processing, background contribution from quartz
243 was removed. Wavelet denoising and baseline correction was carried out by
244 fitting a 6th order polynomial in IRootlab [33, 34].

245

246 2.8 Analysis

247

248 Curve fit of Raman peaks carried out using WIRE 3.4 software. Peak heights
249 were measured of class means of the different time points by curve fitting. For
250 evaluating contributions to different biomolecules the fittings were restricted to

251 the spectral regions of 760-870 cm^{-1} for DNA, 900-980 cm^{-1} for the

252 $v_1PO_4^{3-}$ phosphate region and 1400- 1490 cm^{-1} for the CH$_2$ deformation

253 (extracellular matrix component of collagen). A number of mixed Gaussian-

254 Lorentzian curves were fitted tor each region. Where possible the curve fitting

255 was initiated by using the same number of peaks although these shifted with

256 the time-course. For example at day 3, 9 peaks were selected to deconvolve

257 the phosphate region, but at day 7 and 14 only 7 were needed. These changes

258 reflect the changes in phosphate disorder [35].

259

260 **3. Results and Discussion**

261 **3.1 Assessment of primary calvarial osteoblasts differentiation by**

262 **Raman spectroscopy**

263

264 To assess the differentiation of primary calvarial osteoblasts (COBs) by Raman

265 spectroscopy, osteoblasts were isolated from the calvaria of 4 day old neonate

266 mice by sequential collagenase/EDTA digestion (Figure 1A). Cells were

267 cultured for up to 14 days in standard tissue culture conditions, before fixation

268 with 4% PFA. A single spectrum was collected targeting each cell nucleus. 20

269 spectra were acquired for a cell culture sample. Overall the COBs' Raman

270 spectra are composed of characteristic biomolecular peaks, first assigned by

271 Puppels, now accepted as biomarkers for cells [36]. Spectra were collected

272 within the "Raman fingerprint region" between 600 cm^{-1} – 1750 cm^{-1}. Strong

273 Raman bands were detected for DNA (782 cm^{-1}) and phenylalanine (1004 cm^{-1}

274). The quartz cover slip could have contributed to the background (Figure S1)

275 but the strong Raman signal at 782 cm^{-1} is attributable to the cells. The

276 presence of such a large peak in this region has been previously detected in a

277 number of studies [37-39] A range of protein bands associated with collagen

278 and the extracellular matrix were observed including CH$_2$ deformation at 1450

279 cm^{-1}, Amide III and Amide I [40]. Mineral bands linked with osteoblasts and bone

280 tissue were also detected namely Phosphate v_3 (1030 cm^{-1}) and B-type

281 carbonate (1072 cm^{-1}) as well as weak phosphate bands between 948 and 970

282 cm^{-1}.

283

284 Peak assignment and spectral analysis was carried out on class mean spectra

285 shown in Figure 1C. The class means retain the previously mentioned spectral

286 peaks, highlighted in Figure 1C, and they also display components ascribed to
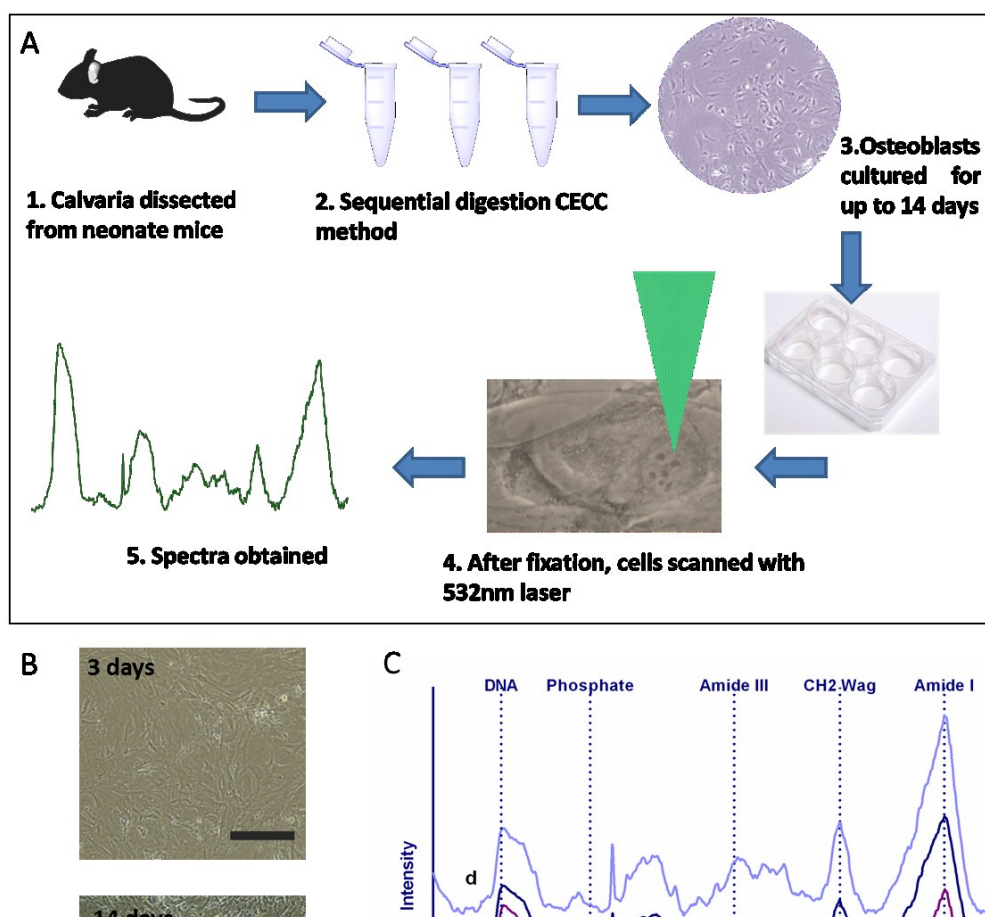

Figure 1. Raman spectroscopy of calvarial osteoblasts (COBs). (A) Schematic of the experimental methodology for this work is shown. Murine calvarial osteoblasts were extracted from 4 day old neonates by sequential collagenase digestion. Cells were cultured up to 14 days on quartz coverslips in standard tissue culture conditions. Following fixation, cell nuclei were scanned with 532 nm laser and spectra obtained from 20 cells per time point. (B) Phase contrast images of COBs in culture highlight phenotypic changes following 14 days of culture in osteogenic media. Scale bar equivalent to 250 μm. (C) Class means of Raman spectra at day 3 (a), 5 (b), 7 (c) and 14 (d). The spectra show differences in key spectral regions over time.

287 mineralised tissue including Amide I, Amide III, CH$_2$ deformation for matrix, and

288 Phosphate v_3 (1030 cm^{-1}) and B-type carbonate (1072 cm^{-1}) bands for mineral

289 [41, 42]. Broad peaks in the phosphate region (948 - 970 cm^{-1}) are also

290 detectable. Before looking at the differences in biochemical composition

291 provided by Raman spectroscopy, we present the results of biological
292 techniques traditionally used to evaluate osteoblast function.
293

294 3.2 **Enzymatic ,mRNA, collagen and DNA measurements of calvarial**
295 **osteoblasts.**
296

297 For assessment of osteoblast maturity and validation of differentiation status,
298 conventional assays and molecular techniques were employed. The Alkaline
299 phosphatase (ALP) activity assay has become the standard assay to measure
300 osteoblast activity *in vitro*. *In vivo*, mature osteoblasts secrete ALP, for which
301 PPi serves as a substrate and when hydrolysed by ALP produces Pi, which
302 accumulates in MVs along with Ca^{2+} during the early phase of mineralisation
303 [21]. *In vitro*, confluent osteogenic cultures are thought to enter an initiation
304 phase after 7 to 14 days, during which time cells will proliferate, express ALP
305 and secrete collagen matrix [43]. The secretion of ALP in osteogenic cultures
306 increases until the cells reach maturation phase and the onset of mineralisation
307 after about 14 – 21 days [23, 43]. Quantitative analysis shows an increase in
308 ALP over time in osteogenic cultures, with the most apparent increase between
309 day 7 and 14 (Fig. 2A).This observation is confirmed by visualisation of ALP
310 activity (Figure 2A; upper panel). Osteoblasts cultured only in basal medium,
311 without the addition of osteogenic mediators (BGP and AA), show little evidence
312 of ALP activity until day 14 of culture. These results highlight that early changes
313 (day 3 to day 7) are not detectable by ALP assay and therefore call for a more
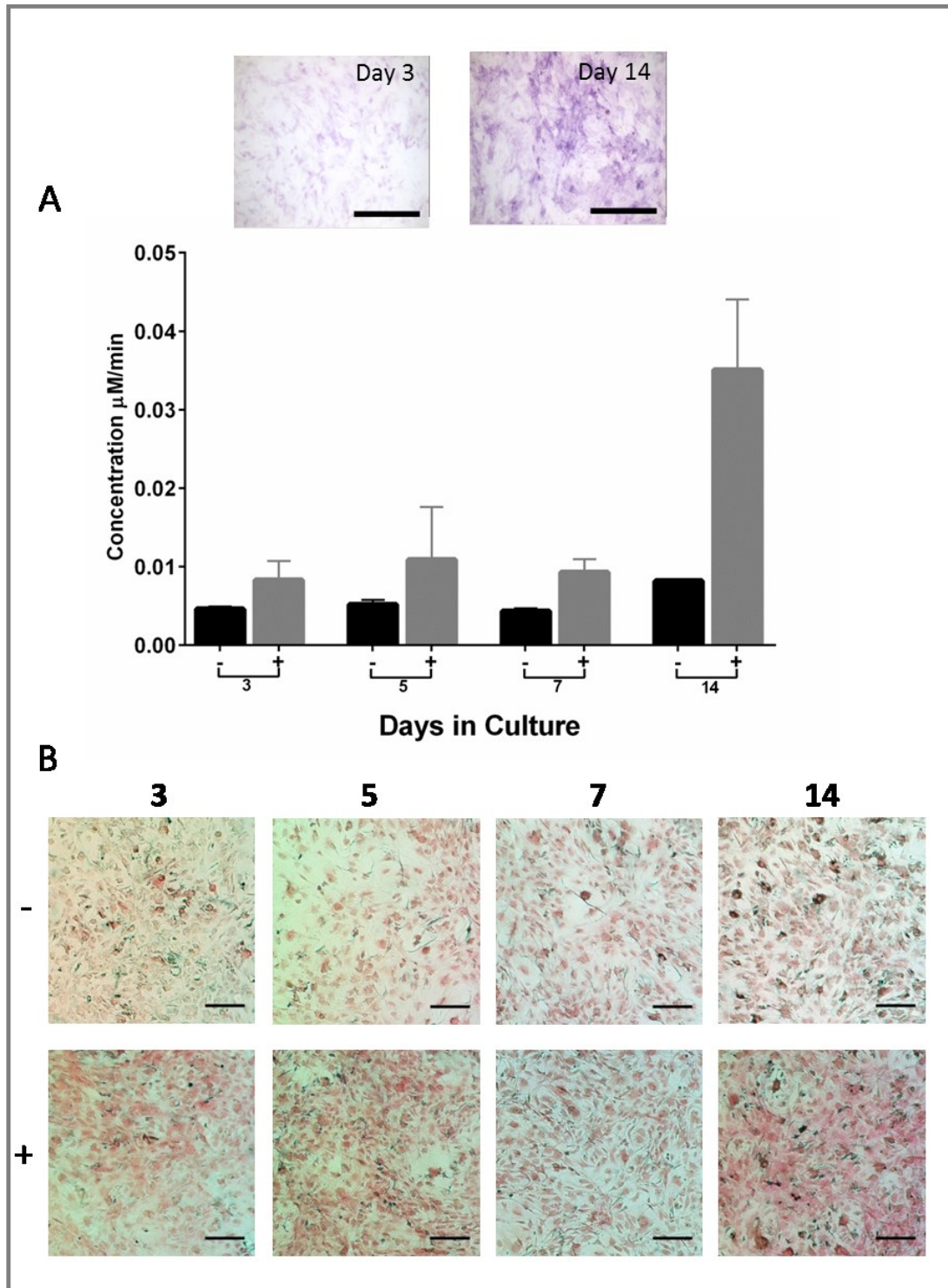314 sensitive approach.
315
316
317
318

10

Figure 2. Alkaline Phosphatase (ALP) activity and Sirius red staining of cultured calvarial osteoblasts (COBs). (A) Results for ALP activity are shown. Cells were cultured in osteogenic (+) or basal medium (-), fixed with 100% ethanol and reacted for ALP and eluted. Data are represented as mean concentration of 2 replicates ± STD. The inset shows exemplar images of cells at Day 3 and Day 14 stained for ALP activity. (B) Images for Sirius red staining of COBs for collagen deposition at indicated time points +/- osteogenic media. Scale bar represents 250 μm.

319

Sirius Red staining for deposited collagen

11

321 To assess the deposition of collagen in the COBs cultures over time, cells
322 cultured with and without osteogenic mediators for 3, 5, 7 and 14 days were
323 stained with Sircol Sirius red dye reagent. After staining cells were visualised
324 using phase contrast microscopy (Figure 2B). No obvious differences were
325 detected over time in the cells cultured in non- osteogenic media (Figure 2B, '-
326 ' row). COBs that were cultured in osteogenic media (Figure 2B '+' row) reveal
327 a fluctuating increase in collagen deposition over time. Nevertheless, at 14 days
328 the COBs cultured in osteogenic media show the most intense and widespread
329 staining, but little difference is discernible between day 3 and day 5 of
330 osteogenic culture.

331

332 **mRNA analysis**
333 To confirm COBs were differentiating as expected, RT² Profiler PCR Array
334 Gene Expression Analysis was carried out. From this array a number of genes
335 were selected to investigate osteogenic commitment by COBs; Col1a1
336 (encodes the major component of collagen type I), SOST (sclerostin, involved
337 in regulation of bone formation in osteoblasts) and ALP (alkaline phosphatase).
338 Interestingly all of these genes show unchanged expression levels between day
339 5 and day 14 (Figure 3A). This data highlights the lack of sensitivity to effectively
340 detect changes in early *in vitro* osteogenesis. It is not unusual to observe
341 increases in enzymatic activity as seen in the ALP assay between day 7 and
342 day 14 (Figure 2A), that are not mirrored in the mRNA expression. This
343 phenomenon of ALP activity not matching mRNA has been previously reported
344 by Weiss *et al* in a study of the sub-epithelial stroma whereby during gestation
345 ALP activity peaked at day 7, but this elevation in enzyme activity was not
346 preceded by induction of mRNA [44]. Although gene expression analysis can
347 provide some insight into early osteogenic behaviour, it is clear that early
348 detection is not always possible and a more sensitive assay is needed to garner
349 an enhanced understanding of osteogenesis.

350

351

352

353

354 **DNA quantitation**

12

355 Early osteogenic commitment is typified by modifications in cellular proliferation.

356 To investigate whether these changes were apparent in our COBs cultures,

357 dsDNA concentration was measured using the Quant-iT™Picogreen® reagent.

358 dsDNA present in genomic DNA isolated from COBs cultured for either 3, 5, 7

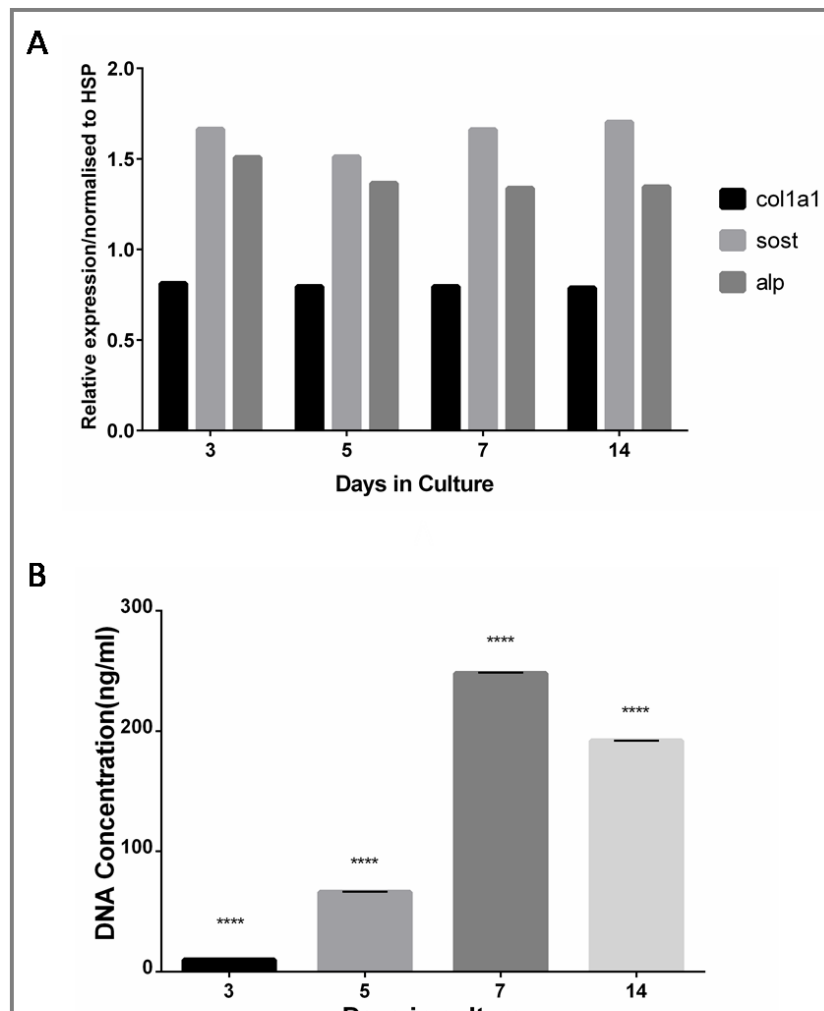359 or 14 days was quantified by the addition of the Picogreen dye. Samples were

Figure 3. Osteogenic gene expression and fluorescence quantitation of DNA of calvarial osteoblasts cultured for up to 14 days. (A) mRNA expression levels of Col1a1, Sclerostin (SOST) and ALP at different time points. They were normalised to HsP. At each desired time point cells were lysed and RNA was isolated from osteoblasts. After generation of cDNA an RT² Profiler PCR Array was performed comprising one sample per well/gene. (B) Quant-iT™Picogreen® fluorescence intensities of dsDNA isolated from COBs. Samples were excited at 480 nm and fluorescence intensity was measured at 520 nm. dsDNA concentration was determined from previously generated standard curve of known DNA concentrations.

360 excited at 480 nm and fluorescence intensity was measured at 520 nm. Figure

361 3B shows the concentration of dsDNA present in each time point, determined

362 from a previously generated standard curve of known DNA concentrations.

363 There is an increase in DNA concentration between day 3 and 5 of COBs

364 culture, indicating a proliferation phase. The DNA concentration continues to

13

365 increase at day 7. At day 14, however, there is a drop in DNA concentration,
366 suggesting the cells have switched to a proliferative state.
367
368 **3.3 Raman spectral changes during early osteogenesis identified by**
369 **univariate deconvolution analysis**
370
371 To assess whether Raman spectroscopy can indeed allow us to detect early
372 biochemical changes in cells, without losing the heterogeneity of the cell
373 population, in this section, we analyse spectral changes evident from the class
374 means (Figure 1C) in more detail.
375 Univariate analysis of class means, revealed a very strong Raman peak at 782
376 cm^{-1} after 3 days of osteogenic COBs culture After 5 days of osteogenic culture,
377 peak intensity decreases, suggesting a drop in DNA concentration. This peak
378 increases between day 7 and day 14. The peak intensities extracted after
379 deconvolution confirms this apparent change in DNA concentration (Figure 4A).
380 In non- osteogenic COBs cultures, deconvolution of peak height intensities
381 revealed that after the initial decrease between day 3 and day 5, very little
382 change is detected between day 5 and day 7, but a considerable increase is
383 shown between day 7 and 14 for the nucleic acid peak at 782 cm^{-1} (Figure S2D).
384 Previous studies have indicated that DNA concentration in cells is related to
385 proliferative status [45, 46]. Our data suggests that COBs are proliferating at
386 first until confluence is reached (at day 5) at which point DNA concentration
387 drops as the cells begin to differentiate. This is in keeping with current
388 understanding of osteoblast behaviour in culture. After isolation, primary
389 osteoblasts will first form collagen matrix and then proliferate on a surface; once
390 confluence is reached, after around 7 days in culture, the fibroblast like pre-
391 osteoblasts start to differentiate into a more mature form of osteoblast [47]. The
392 Picogreen assay showed an increase in DNA concentration until day 7, which
393 coincides with the switch from proliferation to differentiation at day 14 and a
394 decrease in DNA concentration. Osteoblasts reach maturity after 14 days in
395 culture [43]. Analysis of the Raman peaks indicates that after an initial drop in
396 DNA at day 3, there is a gradual increase in proliferation up to day 14. This
397 increase in DNA at day 14 coincides with an increase in extracellular matrix
398 (ECM) associated Raman frequencies (Fig 4B) as well as ALP activity (Fig 2AB

14

399 and an overall increase in phosphate species present (supplementary
400 information Fig. S1). This behaviour suggests the COBs are differentiating and
401 preparing to start mineralising. Mature osteoblasts start to mineralise between
402 21 and 28 days and before that the extracellular matrix (ECM) comprising of
403 mainly collagen is laid down. By targeting the nuclei of individual cells, Raman
404 spectra retain the heterogeneous nature of primary osteoblasts in culture. To
405 isolate DNA from cells, it is necessary to lyse a large number of cells, thereby
406 losing the individual heterogeneity and any subtle variation that might be
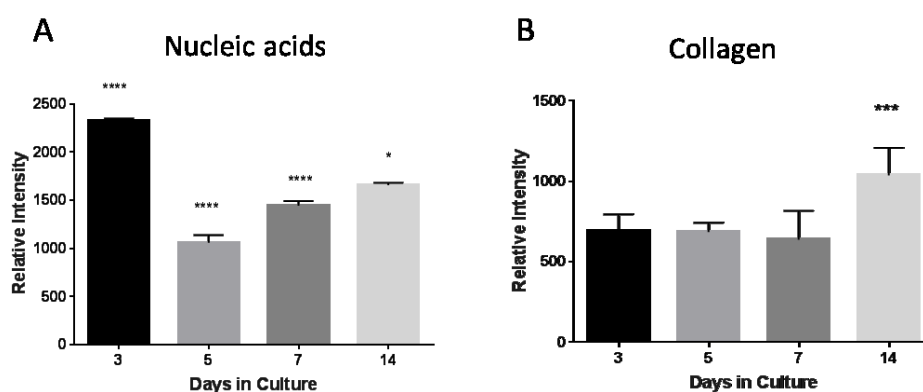407 present in population level concentrations.

Figure 4. Raman spectral data analysis over time for COBs. Peak intensities for (A) Nnucleic acids (782 cm^{-1}) show gradual increase after day 5 of culture and (B) Collagen (CH$_2$ wag 1450 cm^{-1}) showing little change in peak height until day 14 of culture. Spectral deconvolution was carried out on averaged pre-processed spectra of COBs cultured each of the time points. Data is presented as the mean of deconvoluted peak intensity ± SEM (p< 0.05 *** p<0.0001 ****)

408 After 3 days of either osteogenic or non- osteogenic culture, ECM components
409 were detected using Raman spectroscopy. These have been previously
410 described and include bands at 852 cm^{-1} (C-C proline, hydroxyproline), 1003
411 cm^{-1} (phenyalanine ring breathing), 1255 cm^{-1} (Amide III), 1450 cm^{-1} (CH$_2$ wag)
412 and 1660 cm^{-1} (Amide I) [41, 48, 49].
413 The CH$_2$ wag, considered to be a component of collagen, was chosen for further
414 analysis of general matrix production [50-54]. Deconvolution analysis of peak
415 height was carried out on spectra from COBs cultured in osteogenic media.
416 There was no significant change in peak position or intensity in this component
417 of the collagen matrix over the early time points (Figure 4B). There is a
418 significant increase at day 14, which corresponds with increases in phosphate,
419 DNA and ALP activity. This compares well with the results from Sirius Red
420 staining where very little difference was detected in non-osteogenic COBs

15

421 cultures using the Sirius red collagen stain where an increased collagen
422 staining was observed in the osteogenic cultures at day 14, but little difference
423 visible in the early time points. This is similar to that observed with Raman
424 spectroscopy (Figure 4B). The results with the controls (non-osteogenic
425 cultures) are also largely similar in that there is a small increase at Day 14 and
426 at other days over the time course there are little changes. Deconvolution of
427 spectra taken of COBs grown in non- osteogenic medium also shows little
428 change in the CH_2 wag matrix component before day 14 (Figure S2C). Until
429 day 14 the ECM is dominated by a stable collagen component, the presence of
430 the phosphate intermediates indicates that mineralisation has not yet taken
431 place and the matrix is immature.

432

433 3.4 **Raman spectroscopic analysis of phosphates in COBs**

434

435 Osteoblasts ultimately form fully mineralised and mature bone which is primarily
436 calcium hydroxyphosphate (hydroxyapatite or HA). However, before the stable
437 form of hydroxyapatite is reached, a range of calcium phosphate intermediates
438 can be formed. Amorphous calcium phosphate (ACP) is thought to be the first
439 insoluble phase of calcium phosphate [55] This further goes through several
440 intermediate forms and transient mineral species, including carbonated apatite
441 (CAP) and octacalcium phosphate (OCP) before formation of hydroxyapatite
442 (Figure 5).   The presence of transient mineral species has previously been
443 investigated in calvarial cultures and in the formation of bone in vivo [42, 48,
444 49].
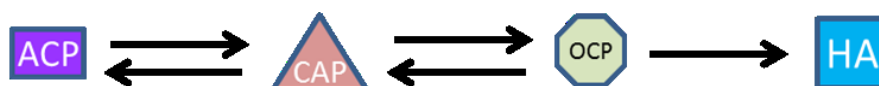
445 **Figure 5. Reaction scheme representing the conversion of amorphous calcium phosphate (ACP) to crystalline
446 hydroxyapatite (HA).** Carbonated apatite (CAP) and octacalcium phosphate (OCP) are postulated as intermediate
447 phosphates. The bi- directional arrows illustrate the transient nature of these phosphate intermediates.

448 In this study, particular attention was paid to the presence of intermediate
449 calcium phosphate species; amorphous calcium phosphate (ACP 945-952 cm^{-1}
450) [42, 49], carbonated apatite (CAP 957-962 cm^{-1}) [41, 49] and octacalcium
451 phosphate (OCP 970 cm^{-1}) [53, 56] (Table 1).

452

16

453 **Table 1. Band assignments for Raman spectra of mineral components.**

Raman Shifts (cm^{-1})	Band assignments	Component
945- 952	PO$_4$, P-O	ACP
955	not detected	OCP
957- 962	v_1 PO$_4$, P-O	CAP
970	v_1 PO$_4$, P-O	OCP

454

455

456 To track the transformation of phosphates from amorphous broad peaks to
457 phosphates with more crystalline properties, deconvolution of peaks was
458 carried out in the the $v_1 PO_4^{3-}$ spectral region between 948 and 970 cm^{-1} (zoomed
459 in phosphate region is shown in Figure S3). While these peaks are not very
460 pronounced their signal-to-noise ratio was >3 and therefore deconvolution was
461 possible, as others have also previously shown [57]. Principal component
462 analysis (PCA) on the phosphate spectral region was also carried out (Figure
463 S3B). It establishes that while there is overlap between different time-points
464 signifying similarity in spectral features there is some segregation (in PC1, PC3
465 and PC4) as well indicating differences between them despite lesser variables
466 (due to the reduced spectral region analysed) in the PCA. Since the differences
467 seem prominent enough in the class means we analysed the differences
468 through deconvolution as described below.

469

470 In osteogenic COBs cultures, deconvolution of peak heights of combined
471 phosphates between 948 cm^{-1} and 970 cm^{-1} show a decrease in phosphate
472 peak height after day 3 (SI Figure S2A). In non- osteogenic COBs cultures,
473 deconvolution of peak heights of combined phosphates show no change
474 between day 3 and day 5. There is a decrease in peak height at day 7, followed
475 by an increase at day 14 (SI figure S2B). More detailed analysis of osteogenic
476 cultures of COBs, revealed that ACP is present with CAP at day 3 compared to
477 other days while OCP is absent. Octacalcium phosphate (OCP) is a well-
478 documented transient precursor to hydroxyapatite [42, 48, 49, 55]. OCP was
479 detected only after 5 days of osteogenic COBs culture, together with a reduction
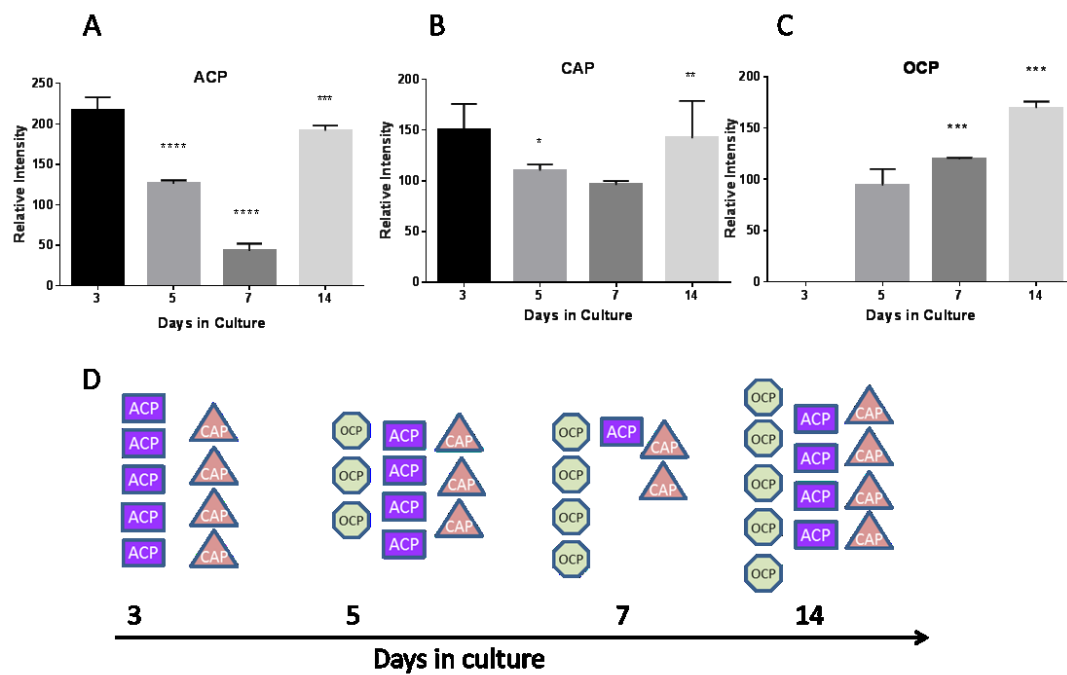480 in ACP and CAP (Figure 6A-C).

17

481

Figure 6. Modifications in phosphate species are evident from 5 days of calvarial osteoblast culture. Deconvolution analysis of phosphate species detected by Raman spectroscopy in COBs reveals alterations in amorphous calcium phosphate (A; ACP), carbonated apatite (B; CAP) and octacalcium phosphate (C; OCP). Data presented as mean of deconvolution ± SEM (p< 0.05 *** p<0.0001 ****). (D) Schematic representation of fluctuating concentrations of intermediate calcium phosphate species.

482 At day 7 of culture there is a significant decrease in ACP, a slight drop in CAP
483 and increased OCP. After 14 days there is a dramatic increase in the presence
484 of all phosphate species. This increase corresponds with a significant increase
485 in ALP activity (Figure 2A), as well as increased collagen deposition (Figure
486 2B). Primary cells are heterogeneous in nature, they are known to contain cell
487 populations at varying degrees of differentiation and maturity [58, 59]. This
488 heterogeneity is evident in Raman spectra obtained from early time points (from
489 day 3 to 5) which show a greater variability owing to differing levels of cell
490 maturity.   This could explain the presence of multiple phosphate species in
491 COBs cultures. COBs are at different stages of differentiation and maturation
492 and therefore differing phosphate species are present simultaneously. It has
493 been suggested that the presence of pre-cursor phosphate species aids in the
494 formation of hydroxyapatite, which could be considered the terminal product of
495 mineral formation and the most stable calcium phosphate salt [60]. Early work
496 by Brown *et al* reported on the existence of octacalcium phosphate (OCP) as a
497 possible intermediate for hydroxyapatite and later went on to characterise the

18

498   Raman band assignment for OCP [56, 61]. Sometimes referred to as β- TCP,

499   OCP is thought to have band positions located at 955 cm^{-1} and 970 cm^{-1}. In

500   their study of calvarial cultures, Crane et al, report on the presence of an OCP

501   like mineral at 955 cm^{-1}, but this mineral is not present in our COBs cultures

502   [42]. An important pitfall was highlighted in a study by Stewart *et al*, where they

503   describe the presence of β-TCP (975 cm^{-1}) in their MC3T3-E1 cell cultures as

504   a consequence of the use of excess β- glycerophosphate [48]. It should be

505   noted that the use of excess β- glycerophosphate (>5 mM) in osteoblast culture

506   can lead to dystrophic mineralisation and impaired cell viability, this could also

507   account for the presence of unexpected phosphate species [23, 62].

508

509

510   **Multivariate analysis of COBs' spectra**

511

512   Multivariate analysis was conducted by means of a pairwise comparison

513   between each time point. Figure 7 represents the 3D scatterplots from the

514   pairwise comparisons. Figure 7A shows the 3D plot of results attained from the

515   PCA of Raman spectra collected from COBs cultured for 5 and 3 days. PC1,

516   PC2 and PC3 represent 64.7%, 24.4% and 3.52% of the variance between the

517   dataset respectively. With exception of one outlier, there is a distinct separation

518   between day 5 and day 3. The PC1 loading (SI figure 4Ai) indicates that the

519   entire spectrum contributes to the group separation between these time points.

520   From the PC2 loading (SI figure 4Aii) Amide I, CH_2 wag and the 782 cm^{-1} peak

521   appear to contribute most to the variance.

522   The 3D scatterplot for results obtained from the PCA of Raman spectra

523   collected from day 7 and day 5 of culture, shows that although the time points

524   remain clearly separated, the loadings are weighted differently this time. PC1

525   accounts for 71.3% of the variance, PC2 for 21.3% and PC3 for just 1.89% of

526   the variance. The PC1 loadings (SI figure 4B i) are very similar to the PC1

527   loadings from day 5 and day 3, however, peaks in the phosphate symmetric

528   stretch region (~950 cm^{-1}), though a small percentage, also contribute to the

19

529 variance in PC1. In PC2 the contribution of peaks in the phosphate symmetric

530 stretch region contribute to a larger percentage of the overall variance.

531

532 The PCA analysis of Raman spectra collected from day 7 and day 14, as

533 revealed by the 3D scatterplot shows the least amount of separation between

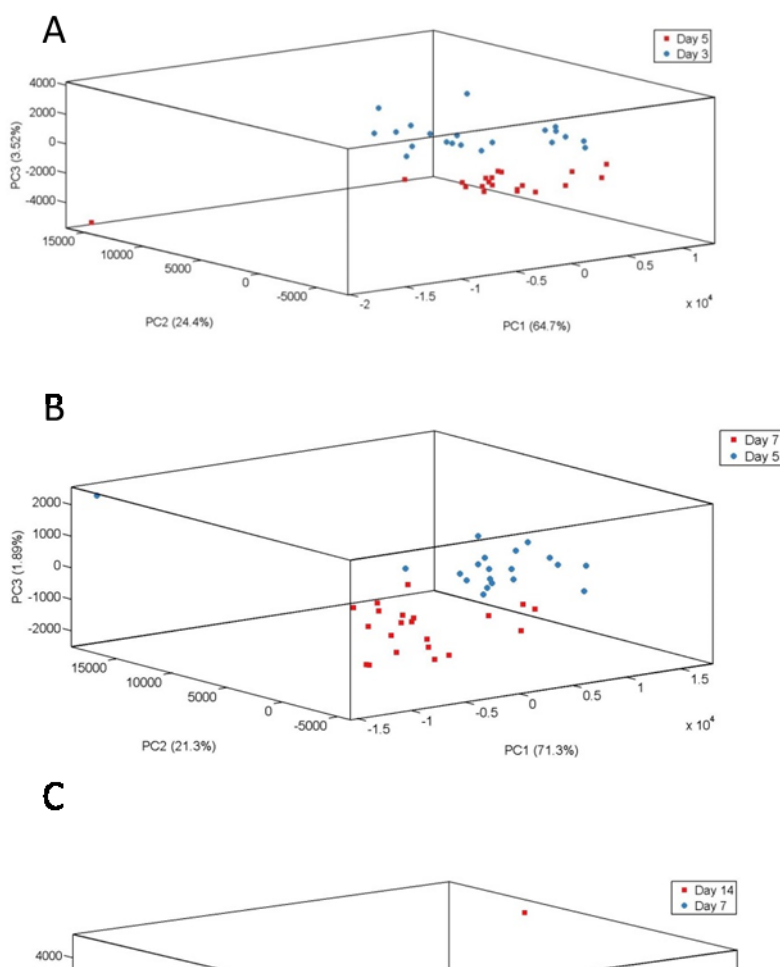534 the groups (Figure 7C). PC1 accounted for 50.5% of variance, PC2 43% and

Figure 7. 3D scatterplots of pairwise PCA analysis output. (A) PCA analysis of day 5 and day 3 spectra of COBs. PC1, PC2 and PC3 represent 64.7%, 24.4% and 3.52% of the variance between the data set respectively. (B) PCA analysis of day 7 and day 5 spectra of COBs. PC1, PC2 and PC3 represent 71.3%, 21.3% and 1.89% of the variance between the data set respectively. (C) PCA analysis of day 14 and day 7 COBs. PC1, PC2 and PC3 represent 50.5%, 43% and 1.96% of the variance between the data set respectively.

535 PC3 1.96%. The components of PC1 are distinguishable as groups, but the

536 components of PC2 are less obvious. It is noteworthy that the results from the

537 ALP assay showed significant increases between cells cultured for 7 and 14

538 days in osteogenic media. The deconvolution analysis of the nucleic acid peak

539 and the 1450 cm^{-1} collagen matrix peak also revealed significant differences

540 between day 7 and 14. The PC1 loading (SI Figure 4Ci) of the PCA output of

20

541 the pairwise comparison between day 7 and 14 indicates that Amide I, CH_2 wag
542 and Amide III contribute to the overall variance. The broad Amide III shoulder
543 is dominated by matrix components. The Amide III shoulder visible in the class
544 mean spectrum of COBs cultured for 14 days in osteogenic media (Figure 1C),
545 appears to be more pronounced at day 14 when compared with day 7,
546 suggesting changes in protein structure over time.

547

548 In general the PCA analysis has confirmed that there are significant differences
549 between COBs cultured over time. Changes in matrix composition and structure
550 contribute to these differences. Changes in the phosphate symmetric stretch
551 were also detected, and appear to contribute to variance, though to a much
552 lesser degree. In most cases the PC loadings indicate a lot of variation over the
553 entire spectrum, and as such the subtle differences are lost. Deconvolution of
554 individual peaks remains most appropriate to detect these subtle changes. The
555 presence of OCP in Raman spectra, could be used as an early marker of
556 osteogenic commitment, detectable before the onset of mineralisation and the
557 appearance of HA. The ability of Raman spectroscopy to detect the presence
558 of OCP before changes are apparent in ALP assay highlights the suitability of
559 this technique to be used as a tool for characterising early cell behaviour.

560

561 **4 Conclusion**

562

563 Our results highlight the ability of Raman spectroscopy to detect subtle changes
564 in osteoblast behaviour in primary cultures shortly after extraction from mice.
565 Where the ALP assay was able to provide some information regarding changes
566 in COBs' activity, by employing Raman spectroscopy, we could characterise a
567 signature of early osteoblast behaviour by quantifying changes in DNA,
568 phosphate species and collagen matrix during different stages of osteogenic
569 commitment. Raman spectroscopy could indicate early changes and provide
570 enhanced information regarding the phenotype of specific osteoblast
571 populations which was not possible using conventional approaches. Whilst
572 Raman spectroscopy could provide a means to assess the direct effects of
573 growing cells on artificial implant substrates, we are not suggesting that the
574 results of this study on quartz are applicable to all implant surfaces. This would,

21

575 however, only be possible if the Raman signals from the implant coatings could
576 be differentiated from the signals generated by the cells or from boney
577 outgrowths prior to osseointegration. Most importantly, if this caveat is taken
578 into account, Raman spectroscopy has shown potential to be used to
579 investigate early markers of differentiation in cells growing on implant coatings.
580 It could be used as a predictor of potential bone outgrowth and osseointegration
581 of these implants *in vivo*, which could lead to improved outcome of artificial
582 implants.
583

588

589 **References**
590

591 1. Lavigne, P., et al., *Involvement of ICAM-1 in bone metabolism: a potential*
592   *target in the treatment of bone diseases?* Expert Opinion on Biological
593   Therapy, 2005. **5**(3): p. 313-320.

594 2. Simon, D.W.N., et al., *Identifying the cellular basis for reimplantation failure*
595   *in repair of the rotator cuff.* Journal of Bone & Joint Surgery, British Volume,
596   2008. **90-B**(5): p. 680-684.

597 3. Wade-Gueye, N.M., et al., *Mice lacking bone sialoprotein (BSP) lose bone*
598   *after ovariectomy and display skeletal site-specific response to intermittent*
599   *PTH treatment.* Endocrinology, 2010. **151**(11): p. 5103-5113.

600 4. Shah, M., et al., *Local origins impart conserved bone type-related differences*
601   *in human osteoblast behaviour.* European cells & materials, 2015. **29**: p. 155-
602   176.

603 5. Zhang, B.G., et al., *Bioactive coatings for orthopaedic implants-recent trends*
604   *in development of implant coatings.* International Journal of Molecular
605   Sciences, 2014. **15**(7): p. 11878-921.

606 6. Nebe, J., et al., *Interface interactions of osteoblasts with structured titanium*
607   *and the correlation between physicochemical characteristics and cell*
608   *biological parameters.* Macromolecular bioscience, 2007. **7**(5): p. 567-578.

22

609   7.   Olivares-Navarrete, R., et al., *Osteoblast maturation and new bone formation*
610   *in response to titanium implant surface features are reduced with age.*
611   Journal of Bone and Mineral Research, 2012. **27**(8): p. 1773-83.

612   8.   Long, F., *Building strong bones: molecular regulation of the osteoblast*
613   *lineage.* Nature Reviews Molecular Cell Biology, 2012. **13**(1): p. 27-38.

614   9.   Komori, T., et al., *Targeted Disruption of Cbfa1 Results in a Complete Lack of*
615   *Bone Formation owing to Maturational Arrest of Osteoblasts.* Cell, 1997.
616   **89**(5): p. 755-764.

617   10.   Ducy, P., et al., *Osf2/Cbfa1: A Transcriptional Activator of Osteoblast*
618   *Differentiation.* Cell, 1997. **89**(5): p. 747-754.

619   11.   Komori, T., *Regulation of osteoblast differentiation by transcription factors.*
620   Journal of cellular biochemistry, 2006. **99**(5): p. 1233-1239.

621   12.   Tonna, S. and N.A. Sims, *Talking among ourselves: paracrine control of bone*
622   *formation within the osteoblast lineage.* Calcified Tissue International, 2014.
623   **94**(1): p. 35-45.

624   13.   Maes, C., et al., *Osteoblast precursors, but not mature osteoblasts, move into*
625   *developing and fractured bones along with invading blood vessels.*
626   Developmental Cell, 2010. **19**(2): p. 329-44.

627   14.   Dirckx, N., M. Van Hul, and C. Maes, *Osteoblast recruitment to sites of bone*
628   *formation in skeletal development, homeostasis, and regeneration.* Birth
629   defects research. Part C, Embryo today : reviews
630   2013. **99**(3): p. 170-91.

631   15.   Roberts, S., et al., *Functional Involvement of PHOSPHO1 in Matrix Vesicle–*
632   *Mediated Skeletal Mineralization.* Journal of Bone and Mineral Research,
633   2007. **22**(4): p. 617-627.

634   16.   Yadav, M.C., et al., *Loss of skeletal mineralization by the simultaneous*
635   *ablation of PHOSPHO1 and alkaline phosphatase function: a unified model of*
636   *the mechanisms of initiation of skeletal calcification.* Journal of Bone and
637   Mineral Research, 2011. **26**(2): p. 286-97.

638   17.   Nahar, N.N., et al., *Matrix vesicles are carriers of bone morphogenetic*
639   *proteins (BMPs), vascular endothelial growth factor (VEGF), and*
640   *noncollagenous matrix proteins.* Journal of Bone and Mineral Metabolism,
641   2008. **26**(5): p. 514-9.

642   18.   Anderson, H.C., *Vesicles associated with calcification in the matrix of*
643   *epiphyseal cartilage. .* The Journal of Cell Biology, 1969. **41**(1): p. 59-72.

644   19.   Millan, J.L., *The role of phosphatases in the initiation of skeletal*
645   *mineralization.* Calcified Tissue International, 2013. **93**(4): p. 299-306.

23

646 20. Golub, E.E., *Biomineralization and matrix vesicles in biology and pathology.*
647   Seminars in Immunopathology, 2011. **33**(5): p. 409-417.

648 21. Stewart, A.J., et al., *The presence of PHOSPHO1 in matrix vesicles and its*
649   *developmental expression prior to skeletal mineralization.* Bone, 2006. **39**(5):
650   p. 1000-1007.

651 22. Taylor, S.E., M. Shah, and I.R. Orriss, *Generation of rodent and human*
652   *osteoblasts.* Bonekey Reports, 2014. **3**: p. 585.

653 23. Orriss, I.R., et al., *Optimisation of the differing conditions required for bone*
654   *formation in vitro by primary osteoblasts from mice and rats.* International
655   journal of molecular medicine
656 2014. **34**(5): p. 1201-8.

657 24. Brauchle, E. and K. Schenke-Layland, *Raman spectroscopy in biomedicine –*
658   *non-invasive in vitro analysis of cells and extracellular matrix components in*
659   *tissues.* Biotechnology Journal, 2013. **8**(3): p. 288-297.

660 25. Buckley, K., et al., *Measurement of abnormal bone composition in vivo using*
661   *noninvasive Raman spectroscopy.* IBMS BoneKEy, 2014. **11**.

662 26. Buckley, K., et al., *Towards the in vivo prediction of fragility fractures with*
663   *Raman spectroscopy.* Journal of Raman Spectroscopy, 2015. **46**(7): p. 610-
664   618.

665 27. McElderry, J.D., et al., *Tracking circadian rhythms of bone mineral deposition*
666   *in murine calvarial organ cultures.* Journal of bone and mineral research
667   2013. **28**(8): p. 1846-54.

668 28. Ghita, A., et al., *Monitoring the mineralisation of bone nodules in vitro by*
669   *space- and time-resolved Raman micro-spectroscopy.* Analyst, 2014. **139**(1):
670   p. 55-8.

671 29. Gentleman, E., et al., *Comparative materials differences revealed in*
672   *engineered bone as a function of cell-specific differentiation.* Nat Mater,
673   2009. **8**(9): p. 763-70.

674 30. Chiang, Y.-H., et al., *Raman spectroscopy for grading of live osteosarcoma*
675   *cells.* Stem Cell Research & Therapy, 2015. **6**(1): p. 1-8.

676 31. McManus, L.L., et al., *Raman spectroscopic monitoring of the osteogenic*
677   *differentiation of human mesenchymal stem cells.* Analyst, 2011. **136**(12): p.
678   2471-81.

679 32. Hung, P.-S., et al., *Detection of osteogenic differentiation by differential*
680   *mineralized matrix production in mesenchymal stromal cells by Raman*
681   *spectroscopy.* PloS one, 2013. **8**(5): p. e65438.

24

682   33.   Trevisan, J., et al., *IRootLab: a free and open-source MATLAB toolbox for*
683   *vibrational biospectroscopy data analysis.* Bioinformatics, 2013. **29**(8): p.
684   1095-1097.

685   34.   Martin, F.L., et al., *Distinguishing cell types or populations based on the*
686   *computational analysis of their infrared spectra.* Nature Protocols, 2010.
687   **5**(11): p. 1748-1760.

688   35.   Awonusi, A., M.D. Morris, and M.M.J. Tecklenburg, *Carbonate Assignment*
689   *and Calibration in the Raman Spectrum of Apatite.* Calcified Tissue
690   International, 2007. **81**(1): p. 46-52.

691   36.   Puppels, G.J., et al., *Studying single living cells and chromosomes by confocal*
692   *Raman microspectroscopy.* Nature, 1990. **347**(6290): p. 301-303.

693   37.   Draux, F., et al., *Raman imaging of single living cells: probing effects of non-*
694   *cytotoxic doses of an anti-cancer drug.* Analyst, 2011. **136**(13): p. 2718-2725.

695   38.   Draux, F., et al., *Raman spectral imaging of single living cancer cells: a*
696   *preliminary study.* Analyst, 2009. **134**(3): p. 542-548.

697   39.   Meade, A.D., et al., *Growth substrate induced functional changes elucidated*
698   *by FTIR and Raman spectroscopy in in–vitro cultured human keratinocytes.*
699   Analytical and Bioanalytical Chemistry, 2007. **387**(5): p. 1717-1728.

700   40.   Carden, A., *Application of Vibrational Spectroscopy to the study of calcified*
701   *tissues.* Journal of Biomedical Optics, 2000. **5**(3): p. 259-268.

702   41.   Mandair, G.S. and M.D. Morris, *Contributions of Raman spectroscopy to the*
703   *understanding of bone strength.* BoneKEy Reports, 2015. **4**: p. 620.

704   42.   Crane, N.J., et al., *Raman spectroscopic evidence for octacalcium phosphate*
705   *and other transient mineral species deposited during intramembranous*
706   *mineralization.* Bone, 2006. **39**(3): p. 434-442.

707   43.   Hoemann, C.D., H. El-Gabalawy, and M.D. McKee, *In vitro osteogenesis*
708   *assays: influence of the primary cell source on alkaline phosphatase activity*
709   *and mineralization.* Pathologie Biologie (Paris), 2009. **57**(4): p. 318-23.

710   44.   Weiss, M., et al., *Analysis of liver/bone/kidney alkaline phosphatase mRNA,*
711   *DNA, and enzymatic activity in cultured skin fibroblasts from 14 unrelated*
712   *patients with severe hypophosphatasia.* American journal of human genetics,
713   1989. **44**(5): p. 686.

714   45.   Short, K.W., et al., *Raman Spectroscopy Detects Biochemical Changes Due to*
715   *Proliferation in Mammalian Cell Cultures.* Biophysical Journal, 2005. **88**(6): p.
716   4274-4288.

25

717   46.   Chan, J.W., et al., *Micro-Raman Spectroscopy Detects Individual Neoplastic*
718   *and Normal Hematopoietic Cells.* Biophysical Journal, 2006. **90**(2): p. 648-656.

719   47.   Cooper, L.F., *Biologic determinants of bone formation for osseointegration:*
720   *Clues for future clinical improvements.* The Journal of Prosthetic Dentistry,
721   1998. **80**(4): p. 439-449.

722   48.   Stewart, S., et al., *Trends in early mineralization of murine calvarial*
723   *osteoblastic cultures: a Raman microscopic study.* Journal of Raman
724   Spectroscopy, 2002. **33**(7): p. 536-543.

725   49.   Tarnowski, C.P., M.A. Ignelzi, and M.D. Morris, *Mineralization of Developing*
726   *Mouse Calvaria as Revealed by Raman Microspectroscopy.* Journal of Bone
727   and Mineral Research, 2002. **17**(6): p. 1118-1126.

728   50.   Rygula, A., et al., *Raman spectroscopy of proteins: a review.* Journal of Raman
729   Spectroscopy, 2013. **44**(8): p. 1061-1076.

730   51.   Wu, Y., et al., *Evaluation of the Bone-ligament and tendon insertions based on*
731   *Raman spectrum and its PCA and CLS analysis.* Scientific Reports, 2017. **7**: p.
732   38706.

733   52.   Salzer, R. and H.W. Siesler, *Infrared and Raman spectroscopic imaging*. 2009:
734   John Wiley & Sons.

735   53.   Inzana, J.A., et al., *Bone fragility beyond strength and mineral density: Raman*
736   *spectroscopy predicts femoral fracture toughness in a murine model of*
737   *rheumatoid arthritis.* Journal of Biomechanics, 2013. **46**(4): p. 723-30.

738   54.   Shea, D.A. and M.D. Morris, *Bone Tissue Fluorescence Reduction for Visible*
739   *Laser Raman Spectroscopy.* Applied Spectroscopy, 2002. **56**(2): p. 182-186.

740   55.   Pompe, W., et al., *Octacalcium phosphate–a metastable mineral phase*
741   *controls the evolution of scaffold forming proteins.* Journal of Materials
742   Chemistry B, 2015. **3**(26): p. 5318-5329.

743   56.   Brown, W.E., *Octacalcium Phosphate and Hydroxyapatite: Crystal Structure of*
744   *Octacalcium Phosphate.* Nature, 1962. **196**(4859): p. 1048-1050.

745   57.   Pezzotti, G., et al., *Raman spectroscopic investigation on the molecular*
746   *structure of apatite and collagen in osteoporotic cortical bone.* Journal of the
747   Mechanical Behavior of Biomedical Materials, 2017. **65**: p. 264-273.

748   58.   Candeliere, G., F. Liu, and J. Aubin, *Individual osteoblasts in the developing*
749   *calvaria express different gene repertoires.* Bone, 2001. **28**(4): p. 351-361.

750   59.   Bianco, P., et al., *Bone sialoprotein (BSP) secretion and osteoblast*
751   *differentiation: relationship to bromodeoxyuridine incorporation, alkaline*

26

752   *phosphatase, and matrix deposition.* Journal of Histochemistry &
753   Cytochemistry, 1993. **41**(2): p. 183-191.

754 60. Koutsopoulos, S., *Synthesis and characterization of hydroxyapatite crystals: a*
755   *review study on the analytical methods.* Journal of biomedical materials
756   research, 2002. **62**(4): p. 600-612.

757 61. Fowler, B.O., M. Markovic, and W.E. Brown, *Octacalcium phosphate. 3.*
758   *Infrared and Raman vibrational spectra.* Chemistry of Materials, 1993. **5**(10):
759   p. 1417-1423.

760 62. Orriss, I.R., S.E.B. Taylor, and T.R. Arnett, *Rat Osteoblast Cultures*, in *Bone*
761   *Research Protocols*, H.M. Helfrich and H.S. Ralston, Editors. 2012, Humana
762   Press: Totowa, NJ. p. 31-41.

763